THE JOURNAL OF PHYSICAL CHEMISTRY A

Article

pubs.acs.org/JPCA

Enhanced Removal of Uranium(VI) by Nanoscale Zerovalent Iron Supported on Na–Bentonite and an Investigation of Mechanism

Gudong Sheng,[†] Xiaoyu Shao,[†] Yimin Li,[†,*] Jianfa Li,[†] Huaping Dong,[†] Wei Cheng,[†] Xing Gao,[‡] and Yuying Huang[‡]

[†]College of Chemistry and Chemical Engineering, Shaoxing University, Huancheng West Road 508, Shaoxing, Zhejiang 312000, P.R. China

[‡]Shanghai Synchrotron Radiation Facility (SSRF), Shanghai Institute of Applied Physics, Chinese Academy of Sciences, Zhangheng Road 239, Shanghai 201204, P.R. China

Supporting Information

ABSTRACT: The reductive removal of U(VI) by nanoscale zerovalent iron (NZVI) was enhanced by using Na^+-saturated bentonite (Na–bent) as the support, and the mechanism for the enhanced removal were investigated comprehensively. Under the same experimental conditions, NZVI supported on the negatively charged Na–bent showed much higher removal efficiency (99.2%) of cationic U(VI) than either bare NZVI (48.3%) or NZVI supported on the positively charged bentonite (Al–bent) did. Subsequent experimental investigations revealed the unique roles of bentonite on enhancing the reactivity and reusability of NZVI. First, Na–bent can buffer the pH in reaction media, besides preventing NZVI from aggregation. Second, Na–bent promoted the mass transfer of U(VI) from solution to NZVI surface, leading to the enhanced removal efficiency. Third, the bentonite may transfer some insoluble reduction products away from the iron surface according to X-ray absorption fine structure (XAFS) study. Finally, Na–bent as the adsorbent to Fe(II) makes it more reactive with U(VI), which enhanced stoichiometrically the reduction capacity of NZVI besides accelerating the reaction rate.

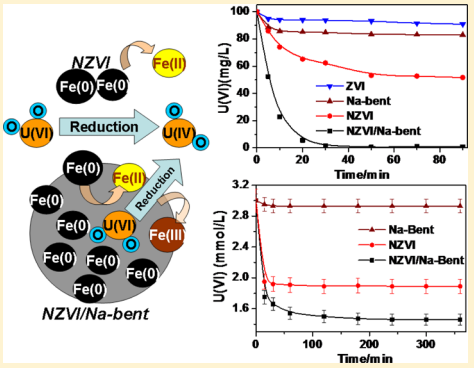

1. INTRODUCTION

Uranium (U) is a common contaminant found in water near many nuclear power plants, weapon-related waste sites and uranium mining locations. It can exist as U(0) or in several oxidation states such as U(III), U(IV), and U(VI), among which U(VI) and U(IV) are the major states in the environment.[1] It is well-known that U(VI) of high toxicity and mobility dominates under oxidizing conditions, and exists mainly as complexed, adsorbed or precipitated uranyl (UO_2^{2+}) species, while U(IV) exists commonly as less soluble species of low toxicity under reducing conditions.[1,2] Many studies have shown that the fate and transport of uranium in the natural environment is greatly affected by the redox transformation between U(VI) and U(IV), and thus reduction of soluble U(VI) to less soluble U(IV) has been proposed as an important method to remediate U-contaminated sites.[1−3]

Since the report of Cantrell et al.,[4] zerovalent iron (ZVI) has been considered as one of the most promising approaches to remediate U(VI) and other metals from contaminated groundwater because ZVI is inexpensive and readily available.[5] Subsequently, numerous studies have focused on the reaction kinetics and mechanisms between ZVI and U(VI).[6,7] Recently, nanoscale zerovalent iron (NZVI) has received much attention for the treatment of U(VI) due to its higher reactivity than ZVI of ordinary sizes.[2,8,9] However, freshly prepared NZVI is apt to aggregate into large clusters, leading to the decreased reactivity.[10] In order to solve this problem, introduction of inert materials into NZVI is an effective tool to prevent its aggregation, and the increased removal of contaminants by NZVI was obtained.[10,11] For this purpose, smectite,[12] resin,[13] silica[11] and carbon nanotubes[10] have been used as the supports of NZVI. In comparison with other support materials, bentonite and its modification products are particularly valuable because they can be tailor-made to achieve the best performance on removing target contaminants.[14−16]

The distinct structure of bentonites make them applicable as templates for synthesizing NZVI particles on clay including the interlayer by reduction of exchangeable Fe(II) or Fe(III). When NZVI is supported on bentonites, its reactivity with target contaminants can be enhanced due to the enrichment of contaminants to solid iron surface.[12] Our previous research indicated that the removal of anionic Cr(VI) and NO_3^- by NZVI was enhanced by using hydroxy-aluminum pillared bentonite (Al–bent) as the support, so was the removal of organic contaminants by organobentonite-supported NZVI.[17−20]

Herein, the reductive transformation of U(VI) to U(IV) by NVZI supported on the Na^+ saturated bentonite (Na–bent)

Received: December 18, 2013
Revised: March 28, 2014
Published: March 28, 2014

was investigated with batch experiments, and compared with that by Al−bent supported NZVI or bare NZVI. The change of pH in the reaction media was monitored, and the reaction products were analyzed with spectroscopic techniques including X-ray photoelectron spectroscopy (XPS) and X-ray absorption fine structure (XAFS). In particular, the role of Fe(II) in the reaction system of NZVI with U(VI) was examined, and a comprehensive mechanism for the enhanced reactivity and reusability of bentonite-supported NZVI was proposed.

2. MATERIALS AND METHODS

2.1. Materials and Chemicals. The original bentonite (Na−bent) primarily composed of Na^+−montmorillonite was purchased from Inner Mongolia, China. The cation exchange capacity (CEC) of Na−bent is determined to be 115 cmol/kg. The hydroxy-aluminum pillared bentonite (Al−bent) was prepared by a cation exchange process with the pillaring solution of poly(hydroxo Al(III)) cations.[15,18] Commercial iron power (ZVI) was purchased from Shanghai Chemical, China, and the grain size passing through a sieve of 100 mesh (<150 μm) was selected and used without further treatment. The chemicals $UO_2(NO_3)_2{\cdot}6H_2O$, HNO_3, NaOH, $FeSO_4{\cdot}7H_2O$, $NaBH_4$, and arsenazo(III) were purchased in analytical purity. All the chemicals were used without any further purification in our experiments. All the solutions were prepared with Milli-Q water under ambient conditions.

2.2. Preparation of NZVI, NZVI/Na−bent and NZVI/Al−bent. The NZVI was prepared with a chemical reduction procedure according to the method described in our previous work.[19,20] Briefly, 250 mL of 0.108 mol/L $NaBH_4$ solution was dropwise added to 0.054 mol/L $FeSO_4{\cdot}7H_2O$ solution until the molar ratio $[BH_4^-]/[Fe^{2+}] = 2.0$ was reached. The solution was stirred for another 30 min under room temperature. The metal particles formed were settled and filtered, and then the solid was washed and finally vacuum-dried. The bentonite-supported NZVIs (NZVI/Na−bent and NZVI/Al−bent) were prepared by a similar procedure as described above, except that 8.00 g of Na−bent or Al−bent was soaking in 250 mL of 0.054 mol/L $FeSO_4{\cdot}7H_2O$ solution under continuous stirring.[17,18]

ζ potential was measured by nano-ZS model (Malvern) ζsizer instrument. X-ray diffraction (XRD) measurement was performed with a Rigaku D/MAX-2500 system using Cu Ka radiation at 0.1542 nm. The Brunauer−Emmett−Teller (BET) specific surface areas were obtained from nitrogen adsorption data at 77 K in a Micromeritics ASAP 2020 system. The samples were degassed at 300 ∘C under vacuum prior to the measurement. Transmission electron microscope (TEM) images were obtained in a JEM-1010 instrument using an accelerating voltage of 80 kV. The iron content was measured with the atom absorption spectrophotometry in a Shimadzu AA-6300 Spectrophotometer.[19]

2.3. Batch Experiment for U(VI) Removal. Typically, four iron samples including ZVI (0.00548 g), NZVI (0.0100 g), NZVI/Al−bent (0.0248 g), and NZVI/Na−bent (0.0246 g) was added into a 150 mL conical flask containing 100 mL of U(VI) solution with certain initial concentration (C_o) under stirring. In these treatments, the four iron samples were used at the same dosage of iron of 0.0500 g/L. Al−bent (0.0198 g) and Na−bent (0.0196 g) alone were also used in a separate treatment, and the bentonites' dosages were the same as those used in the NZVI/Al−bent and NZVI/Na−bent treatments. The U(VI) solution was deoxygenated by N_2 stream for 10 min before adding iron samples, and kept sealed with stopper during the reaction. The removal experiment was carried out by putting in the flask in a thermostatic shaker bath at 25 ± 0.5 °C for 90 min, with a rotation speed of 250 rpm. At the given time intervals, 1 mL solution aliquots were withdrawn and filtered through a 0.22 μm filtering membrane. The concentration of U(VI) at time t (C_t) was determined by arsenazo(III) spectrophotometric method at 650 nm. The removal efficiency of U(VI) was calculated as removal efficiency (%) = $(C_0 - C_t)/C_0 \times 100\%$. The data of batch experiments were obtained in triplicates.

The stability and reusability of iron samples during U(VI) removal was evaluated by repetitive experiments as following: 100 mL U(VI) solution was mixed with a certain amount of NZVI, NZVI/Al−bent, and NZVI/Na−bent. After 120 min, 1 mL solution was withdrawn from the flask for analysis of U(VI) concentration, and then an additional 1 mL U(VI) solution with a proper concentration was added. For this purpose, the U(VI) concentration and pH remained the same at the beginning of each of the four cycles.

2.4. Adsorption of U(VI) on Na−bent and Al−bent. The adsorption isotherms were determined by bath equilibrium of 20 mg of Na−bent or Al−bent with 100 mL of U(VI) solutions with varied initial concentrations. The adsorption experiments were carried out in a thermostatic shaker bath at 25 ± 0.5 °C for 90 min. After equilibrium, the liquid samples were filtered through a 0.22 μm membrane, and then the equilibrium concentration of U(VI) were measured. The adsorbed amount (Q_e) was calculated from the difference between the initial (C_0) and the equilibrium (C_e) concentrations of U(VI).

2.5. Spectroscopic Experiments. The samples for the spectroscopic experiments were prepared as following: a 500 mL solution containing 100 mg/L U(VI) was mixed with a certain amount of Na−bent (0.0980 g), NZVI (0.0500 g), and NZVI/Na−bent (0.1230 g). After 120 min, the solid particles were filtered, then washed, and finally dried. The details for the collection of XPS and XAFS spectra are presented in Text S1 in Supporting Information.

3. RESULTS AND DISCUSSION

3.1. Characterizations of Iron Samples. X-ray diffraction (XRD) pattern showed that NZVI, NZVI/Al−bent, and NZVI/Na−bent are dominantly composed of zerovalent ion (Fe^0), which were characterized by the main reflection at 44.8°.[17] The morphology of NZVI, NZVI/Al−bent, and NZVI/Na−bent was observed by transmission electron microscope (TEM). As shown in Figure SM-1, the bare NZVI (Figure SM-1A) exists as necklace-like aggregation, while NZVI/Al−bent (Figure SM-1B) or NZVI/Na−bent (Figure SM-1C) were clearly discrete and well dispersed on the Al−bent or Na−bent carrier.[17,18] This indicated that the NZVI particles supported on such carriers could avoid aggregating. The specific surface areas of these samples were determined to be 0.35 m^2/g for ZVI, 32.6 m^2/g for NZVI, 31.8 m^2/g for NZVI/Na−bent, and 46.9 m^2/g for NZVI/Al−bent. The iron contents of ZVI, NZVI, NZVI/Al−bent, and NZVI/Na−bent were measured to be 91.2%, 53.1%, 21.1%, and 23.3%, respectively. Besides this, the sodium contents of Na−bent before and after immobilization of NZVI were measured to be 2.50% and 0.23%, respectively. The steep decrease of sodium content was due to the ion exchange of some Na^+ ions from the bentonite with Fe^{2+} ions.

dx.doi.org/10.1021/jp412404w | J. Phys. Chem. A 2014, 118, 2952−2958

3.2. Enhanced Removal of U(VI) by the Bentonite-Supported NZVI. Figure 1 shows the reductive removal

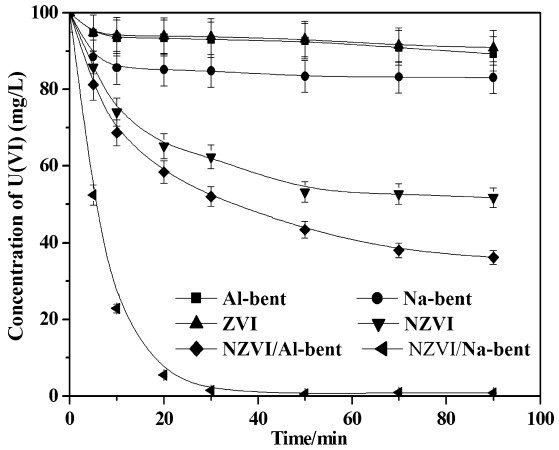

Figure 1. Removal efficiencies of U(VI) by various iron samples.

efficiency of U(VI) by the four iron samples, including ZVI, NZVI, NZVI/Al−bent, and NZVI/Na−bent at the same initial iron content (100 mg/L). The contribution of adsorption by the bentonites (Al−bent and Na−bent) was also determined at the same bentonite dose as those used in the NZVI/Al−bent and NZVI/Na−bent treatments. As can be seen, the removal efficiency of U(VI) by ZVI is only 9.08% after 90 min, which is much lower than that by NZVI (48.3%). The higher reactivity of NZVI is related to its smaller size of iron particles.[21] In addition, the removal efficiency of U(VI) by NZVI/Al−bent and NZVI/Na−bent reached 65.6% and 99.2% after 90 min, respectively, both are much higher than that by bare NZVI (48.3%), indicating the increased reactivity of NZVI by supporting it on the bentonites (Al−bent and Na−bent). Particularly, U(VI) was almost completely removed in the NZVI/Na−bent treatment, the removal efficiency (99.2%) is not only higher than that by bare NZVI (48.3%), but also superior to the sum (65.2%) of the reduction by NZVI plus the adsorption by Na−bent (16.9%), indicating a synergetic effect between adsorption by Na−bent and reduction by NZVI.

First, the enhanced reactivity of the bentonite-supported NZVI (NZVI/Al−bent and NZVI/Na−bent) is related to the dispersion of NZVI particles in the supports (Figure SM-1B and SM-1C), which provides both NZVI/Al−bent and NZVI/Na−bent with more accessible reactive sites for reduction of U(VI) than the aggregated NZVI (Figure SM-1A). Second, the enhancement of NZVI reactivity by supporting on the bentonites may be explained with a surface mediated reaction mechanism, in which the removal efficiency of U(VI) is related to the concentration of U(VI) in the vicinity of iron surface. So a solid surface favorable for adsorption of U(VI) may be beneficial for its reduction by NZVI. According to the adsorption isotherms of U(VI) on Na−bent and Al−bent (Figure 2A), both bentonites can adsorb a certain amount of U(VI), thus the concentration of U(VI) in the solid surface increased, which facilitated the mass transfer of U(VI) from aqueous to iron surface, and accelerated the reduction rate of U(VI) in the supported NZVI systems. More importantly, we can see from Figure 2A that the adsorption capacity of U(VI) on Na−bent is much higher than that on Al−bent. Therefore, more U(VI) can be enriched on NZVI/Na−bent, leading to the higher removal of U(VI).

The higher adsorption of U(VI) by Na−bent is related to its surface electrical property, as indicated by surface ζ potentials of the two bentonites determined at a pH range from 2.0 to 10.0 (Figure 2B). It can be seen that, Na−bent exhibits negative ζ potentials in this pH range, indicating a negatively charged surface of Na−bent. Otherwise, the ζ potentials of Al−bent are positive at pH below pH_{PZC} (the pH_{PZC} of Al−bent is ~7.8), indicating that the surface of Al−bent is positively charged at pH < 7. The results are similar to previous reports.[22,23] Therefore, under our experimental condition (pH < 7), the negatively charged Na−bent favors the adsorption of cationic species such as UO_2^{2+} (U(VI)), whereas the positively charged Al−bent tends to adsorb more anionic species such as Cr(VI) and NO_3^-. As a result, a more efficient removal of the cationic contaminant (U(VI)) was obtained in the NZVI/Na−bent treatment, while the NZVI/Al−bent composite is more powerful in remediation of some anionic contaminants.[18,19]

3.3. Kinetic Study on U(VI) Removal by NZVI Samples. To study the kinetics of U(VI) removal by iron samples, the removal of U(VI) by NZVI, NZVI/Al−bent, and NZVI/Na−bent was conducted as a function of initial U(VI) concentration (25, 50, 100, and 200 mg/L), and the results are shown in Figure SM-2. The removal efficiency of U(VI) by the iron samples is in the order of NZVI/Na−bent > NZVI/Al−bent > NZVI at various initial concentration. The Langmuir−Hinshelwood (L-H) model was employed to investigate the kinetics of U(VI) removal by the iron samples.[24]

$$\frac{1}{r_0} = \frac{1}{k_1 k_2} \times \frac{1}{C_0} + \frac{1}{k_1}$$

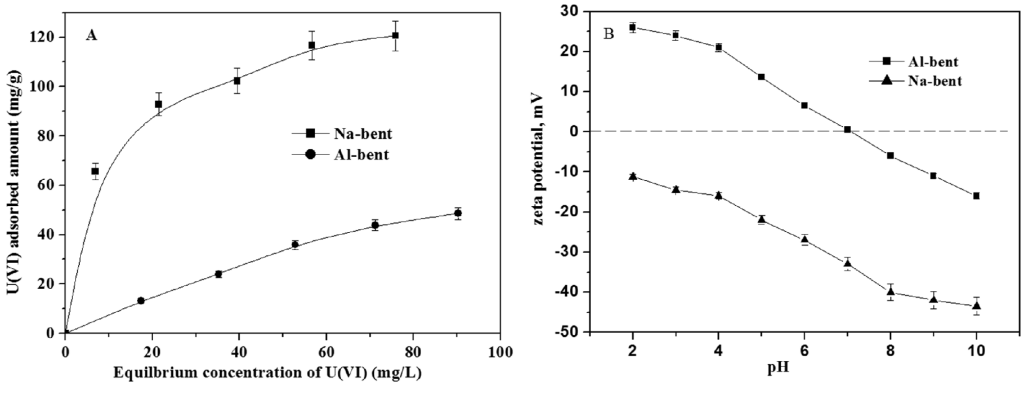

Figure 2. (A) Adsorption isotherms of U(VI) on Na−bent and Al−bent. (B) ζ potential of Na−bent and Al−bent as a function of solution pH.

dx.doi.org/10.1021/jp412404w | J. Phys. Chem. A 2014, 118, 2952−2958

Table 1. Parameters for Kinetics of Uranium Reduction

treatment	fitted equation	k_1 (mmol/(L min))	k_2 (L/mmol)	R
NZVI	$\frac{1}{r_0} = 29.704 + 21.399\frac{1}{C_0}$	0.0337	1.39	0.999
NZVI/OH-Al−bent	$\frac{1}{r_0} = 19.307 + 11.636\frac{1}{C_0}$	0.0518	1.66	0.996
NZVI/Na−bent	$\frac{1}{r_0} = 12.717 + 3.700\frac{1}{C_0}$	0.0786	3.44	0.998

where r_0 is the initial reaction rate, C_0 is the initial concentration of U(VI), k_1 is the reaction rate constant, and k_2 is the adsorption coefficient. As shown in Table 1, the reaction rate constant (k_1) and the adsorption coefficient (k_2) for the NZVI/Na−bent treatment was 2 times and nearly 2.5 times larger than that for the NZVI alone, respectively. In comparison, both k_1 and k_2 for the NZVI/Al−bent treatment was smaller than that for the NZVI/Na−bent. These results indicated that the reaction rate of U(VI) with NZVI was accelerated by Na−bent, and confirmed the synergetic effect between adsorption by Na−bent and reduction by NZVI. The reaction rate was positively related to the adsorbed amount of U(VI) on iron samples.

3.4. Enhanced Stability of the Supported NZVI. The repeated availability of the different forms of NZVI after many cycles is very important for their practical application. According to the recycling experiments of U(VI) removal by NZVI, NZVI/Na−bent and NZVI/Al−bent (Figure 3), we

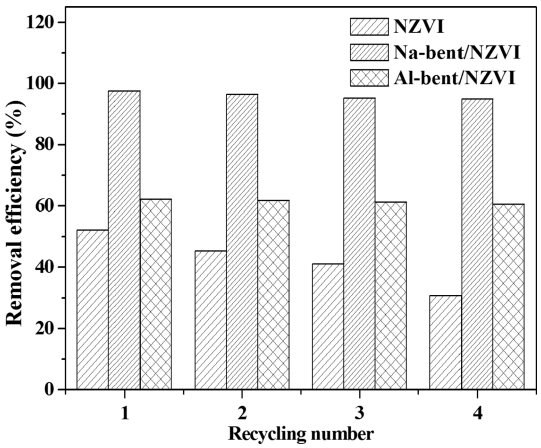

Figure 3. Recycling for the removal of U(VI) by NZVI, NZVI/Al−bent, and NZVI/Na−bent.

found that the removal of U(VI) by the bare NZVI decreased from 52.2% to 30.8% after four cycles, however, the removal of U(VI) only decreased from 62.2% to 60.5% in NZVI/Al−bent treatment and from 97.5% to 94.9% in NZVI/Na−bent treatment, respectively. The results indicate that bentonite-supported NZVIs displayed much higher stability and reusability than the bare NZVI, which is partly due to a certain amount of NZVI intercalated in the interlayer of bentonites and not readily available for oxidization. Besides, the higher stability of the bentonite-supported NZVIs is related to the particular functional groups in the bentonites. Figure 4 showed the variation of pH during reaction of U(VI) with NZVI, NZVI/Al−bent, and NZVI/Na−bent at initial pH =4.0. The results indicated that the introduction of Al−bent and Na−bent as the support materials could help maintain a lower pH in both

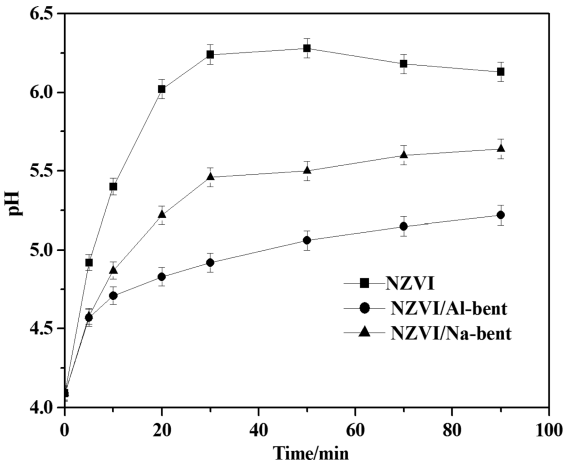

Figure 4. Variation of pH during the reaction process of U(VI) by NZVI, NZVI/Al−bent, and NZVI/Na−bent.

NZVI/Al−bent (~5.0) and NZVI/Na−bent (~5.5) treatment systems than that in NZVI system (~6.2). This is probably attributed to the buffering effect of aluminol or silanol groups on the bentonites.[25,26] As pH increased with H^+ being consumed, the aluminol or silanol groups dissociated to compensate the depletion of H^+. So, the reaction pH of the bentonite-supported NZVIs was much lower and the corrosion products, i.e., iron (hydr)oxides, were reduced, thus the reactive sites on the solid iron surface became more accessible by U(VI) ions.

3.5. Analysis of Reaction Products. 3.5.1. XPS Results. The chemical compositions of the solid products after reaction were analyzed by XPS. As can be seen from Figure SM-3, the $U_{4f7/2}$ and $U_{4f5/2}$ peaks are located at around 380 and 390 eV for the NZVI (Figure SM-3A) and NZVI/Na−bent (Figure SM-3B) samples, respectively. In order to determine the relative proportions of U(VI) and U(IV), curve fitting of the U_{4f} photoelectron peaks was performed according to the method of Schinder et al.,[27] and the results are shown in Table 2. The relative proportions of U(VI) and U(IV) were 66.1%

Table 2. Results of Decomposed Peaks from U 4f

treatment	U^{IV}/%	U^{VI}/%	U^{IV}/U^{VI}
NZVI	33.9	66.1	0.5
NZVI/Na−bent	69.7	30.3	2.3

and 33.9% for NZVI, and 30.3% and 69.7% for NZVI/Na−bent, respectively. This indicated that using Na−bent as the support, except for the enhanced removal efficiency and reaction rate of U(VI) by NZVI, the reductive transformation of U(VI) into less soluble and toxic U(IV) by NZVI could be also enhanced.

dx.doi.org/10.1021/jp412404w | J. Phys. Chem. A 2014, 118, 2952−2958

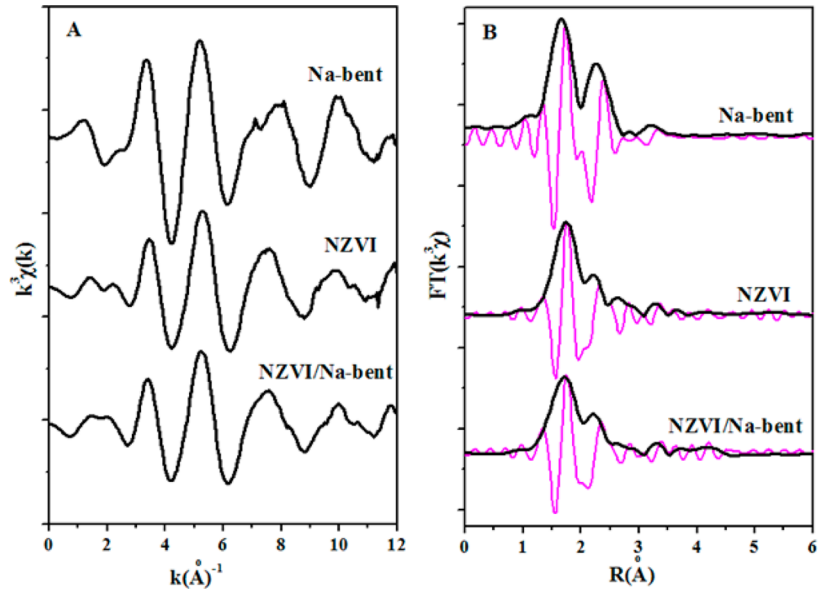

Figure 5. EXAFS spectra of U L_{III} from Na–bent, NZVI, and NZVI/Na–bent reactions with U(VI).

3.5.2. XAFS Results. Information on the local environment of U atoms in the reaction samples is provided by analysis of the EXAFS data. The U L_{III}-edge background-subtracted, k^3-weighted $\chi(k)$ data and the corresponding Fourier transformed EXAFS data from the reaction samples are shown in Figure 5, and the fitting results are shown in Table 3. For the samples of U(VI)-treated Na–bent, the obtained fit results, i.e. 2.0 O_{ax} at ∼1.78 Å, 5.6 O_{eq} at ∼2.38 Å and 2.0 Al/Si at ∼3.65 Å, indicate that U(VI) forms inner-sphere surface complexes on Na–bent. The photoelectron backscattering function of Al and Si are similar, and thus it is not possible to use EXAFS spectra to distinguish between Al and Si atom. The EXAFS data for U(VI)-treated NZVI show two coherent U–O shell composed of ∼1.4 O atoms at ∼1.73 Å and ∼7.5 O atoms at ∼2.36 Å (U–O_1 shell), whereas fitting the U(VI)-treated NZVI/Na–bent show only one U–O shell composed of ∼0.6 O atoms at ∼1.73 Å and ∼7.8 O atoms at ∼2.36 Å. The U–O distance of 1.73 Å accounts for the U–O_{ax} shell of U(VI), while the U–O distance of 2.36 Å is typical for the U–O_1 shell in U(IV) (UO_2) and for the U-O_{eq} shell of U(VI) (UO_2^{2+}). According to the approach reported by O'Loughlin et al.,[28] the amounts of U(VI) can be estimated from the coordination number (CN) for the U–O_{ax} shell, assuming that U(VI) is present as uranyl (UO_2^{2+}) with 2O_{ax}. This approach yields a fraction of U(VI) of ∼70% and U(IV) of ∼30% in the NZVI sample, while ∼30% of U(VI) and ∼70% of U(IV) can be estimated in the NZVI/Na–bent sample, the result was in agreement with the XPS result. The number of U–O_1 was constrained to 8 based on the coordination environment of U(IV) in UO_2. Besides, we can also see ∼7.2 U atoms at ∼3.83 Å for NZVI sample and ∼7.6 U atoms at ∼3.84 Å for NZVI/Na–bent sample, indicating the formation of UO_2.[29] The presence of U–Fe signal (1.8 Fe at ∼3.44 Å) in the NZVI sample indicates that some of the U products are in intimate association with NZVI. Of particular significance is the presence of U–Al/Si signal (1.6 Al/Si at ∼3.58 Å) in the NZVI/Na–bent sample, suggesting that some less soluble U products produced may be transferred to the surface of Na–bent, which is an important factor for the enhanced reactivity and stability of NZVI by the introduction of Na–bent as support material.

Table 3. EXAFS Results of Reacted Samples at U L-edge

treatment	shell	R (Å)	N	σ^2 (Å^2)
Na–bent	U–O_{ax}	1.78 ± 0.02	2.0 ± 0.1	0.012
	U–O_{eq}	2.38 ± 0.02	5.6 ± 0.2	0.015
	U–Al/Si	3.65 ± 0.03	2.0 ± 0.1	0.022
NZVI	U–O_{ax}	1.73 ± 0.02	1.4 ± 0.2	0.018
	U–O_1	2.36 ± 0.01	7.5 ± 0.3	0.031
	U–Fe	3.44 ± 0.03	1.8 ± 0.2	0.028
	U–U	3.83 ± 0.04	7.2 ± 0.4	0.034
NZVI/Na–bent	U–O_{ax}	1.73 ± 0.01	0.6 ± 0.2	0.018
	U–O_1	2.36 ± 0.02	7.8 ± 0.1	0.015
	U–Al/Si	3.58 ± 0.03	1.6 ± 0.2	0.036
	U–U	3.84 ± 0.02	7.6 ± 0.3	0.038

3.6. Role of Fe(II) Adsorbed on NZVI/Na–bent Composite in U(VI) Removal. As a further investigation on the mechanism of enhanced removal of U(VI) by NZVI/Na–bent, an experiment was conducted on the reaction of 3 mmol/L U(VI) with NZVI or NZVI/Na–bent containing 1 mmol/L iron, in a pH = 5.5 buffer solution (the pH value is similar to that of after NZVI/Na–bent reaction with U(VI)). According to the results shown in Figure 6, we can calculate that only 1.1 mmol of U(VI) was reduced by NZVI containing 1 mmol iron, while 1.5 mmol of U(VI) was removed by NZVI/Na–bent at the same dose of iron. This indicates that the reduction of U(VI) by per unit mass of iron can be increased by supporting NZVI on Na–bent; namely, the reduction capacity of iron was stoichiometrically increased by nearly 1.5 times.

According to the above calculation, an stoichiometric reduction of U(VI) by NZVI can be described with eq 1.

$$UO_2^{2+} + Fe \rightarrow UO_2 + Fe^{2+} \quad (1)$$

The increased reduction capacity of NZVI/Na–bent should be related to Fe(II) ions in the composite system, which can reduce more U(VI) as described in eq 2. So the reaction of U(VI) with iron of NZVI/Na–bent composite can be presented as a stoichiometric equation as eq 3.

dx.doi.org/10.1021/jp412404w | J. Phys. Chem. A 2014, 118, 2952–2958

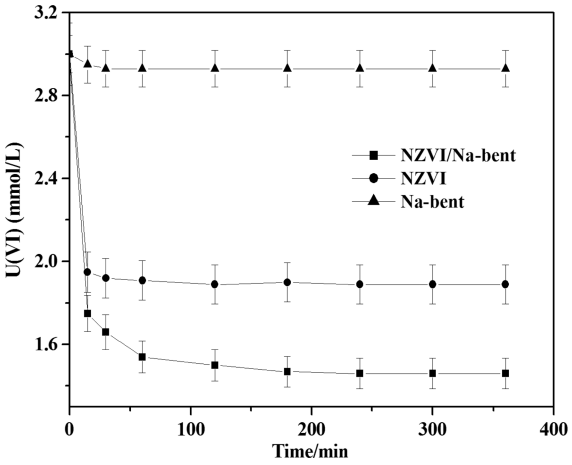

Figure 6. Results of the reaction of 3 mmol/L U(VI) with NZVI or NZVI/Na–bent containing 1 mmol/L iron, in a pH = 5.5 buffer solution.

$$UO_2^{2+} + 2Fe^{2+} \rightarrow UO_2 + 2Fe^{3+} \quad (2)$$

$$3UO_2^{2+} + 2Fe \rightarrow 3UO_2 + 2Fe^{3+} \quad (3)$$

This suggested reaction mechanism is consistent with a recent study, in which Chakraborty et al. found that the reactivity of Fe(II) adsorbed on montmorillonite was much higher than that of free Fe(II) in aqueous solution, and could act as a reductant for U(VI).[30] Charlet et al. studied the reactivity of Fe(II) adsorbed on montmorillonite to Se(IV), and observed slow reduction of Se and formation of a solid phase on montmorillonite surface.[31] Jaisi et al. found that Tc(VII) could be effectively reduced by Fe(II) adsorbed on nontronite.[32] In this NZVI/Na–bent system, the Fe(II) formed may be adsorbed on the negatively charged Na–bent, which makes Fe(II) more reactive with U(VI). However, the reason for the higher reactivity of adsorbed Fe(II) needs to be further investigated.

4. CONCLUSIONS

In conclusion, the bentonites play multiple roles when they are used as the support of NZVI besides dispersing iron nanoparticles, which makes the bentonites superior to other support materials on enhancing the reactivity of NZVI. In this work, the negatively charged surface of Na–bent makes it a better choice as the support of NZVI for removing cationic U(VI). The synergetic effect between Na–bent and NZVI observed in batch removal experiments was confirmed by kinetic studies, that is, the adsorption by Na–bent facilitated the mass transfer of U(VI) from aqueous to iron surface, and then accelerated the reduction of U(VI) by NZVI. Beyond this, the bentonites exhibited obvious pH buffering during the reaction, and could transfer the insoluble reduction products away from the iron surface, resulting in the improved stability and reusability of NZVI. The most interesting role of Na–bent is that it could stoichiometrically enhance reactive capacity of NZVI with U(VI), i.e. one mole of iron in the NZVI/Na–bent can reduce 1.5 mol of U(VI), which is almost 1.5 times higher than that of bare NZVI. In view of these particular roles of Na–bent, NZVI/Na–bent is obviously advantageous on removing U(VI) in environment.

■ ASSOCIATED CONTENT

Supporting Information

Details of XPS study and XAFS measurements, TEM images, kinetics studies, and XPS spectra. This material is available free of charge via the Internet at http://pubs.acs.org.

■ AUTHOR INFORMATION

Corresponding Author

*(Y.L.) Telephone: +86 575 8834 2386. Fax: +86 575 8831 9253. E-mail: liym@usx.edu.cn.

Notes

The authors declare no competing financial interest.

■ ACKNOWLEDGMENTS

This work was supported by the National Natural Science Foundation of China (21177088 and 201207092).

■ REFERENCES

(1) Jang, J. H.; Dempsey, B. A.; Burgos, W. D. Reduction of U(VI) by Fe(II) in the presence of hydrous ferric oxide and hematite: Effects of solid transformation, surface coverage, and humic acid. *Water Res.* **2008**, *42*, 2269–2277.

(2) Yan, S.; Hua, B.; Bao, Z. Y.; Liu, C. X.; Deng, B. Uranium (VI) removal by nanoscale zerovalent iron in anoxic batch systems. *Environ. Sci. Technol.* **2010**, *44*, 7783–7789.

(3) Liger, E.; Charlet, L.; Van Cappellen, P. Surface catalysis of uranium(VI) reduction by iron(II). *Geochim. Cosmochim. Acta* **1999**, *63*, 2939–2955.

(4) Cantrell, K. J.; Kaplan, D. I.; Wietsma, T. W. Zero-valent iron for the in situ remediation of selected metals in groundwater. *J. Hazard. Mater.* **1995**, *42*, 201–212.

(5) Liang, L.; Yang, W.; Guan, X.; Li, J.; Xu, Z.; Wu, J.; Huang, Y.; Zhang, X. Kinetics and mechanisms of pH-dependent Se(IV) removal by zero valent iron. *Water Res.* **2013**, *47*, 5846–5855.

(6) Farrell, J.; Bostick, W. D.; Jarabek, R. J.; Fiedor, J. N. Uranium removal from ground water using zero valet iron media. *Ground Water* **1999**, *37*, 618–624.

(7) Noubactep, C.; Schöner, A.; Meinrath, G. Mechanism of uranium removal from the aqueous solution by elemental iron. *J. Hazard. Mater.* **2006**, *132*, 202–212.

(8) Crane, R. A.; Dickinson, M.; Popescu, I. C.; Scott, T. B. Magnetite and zero-valent iron nanoparticles for the remediation of uranium contaminated environmental water. *Water Res.* **2011**, *45*, 2931–2942.

(9) Dickinson, M.; Scott, T. B. The application of zero-valent iron nanoparticles for the remediation uranium-contaminated waste effluent. *J. Hazard. Mater.* **2010**, *178*, 171–179.

(10) Lv, X.; Xu, J.; Jiang, G.; Xu, X. Removal of chromium(VI) from wastewater by nanoscale zero-valent iron particles supported on multiwalled carbon nanotubes. *Chemosphere* **2011**, *85*, 1204–1209.

(11) Zheng, T.; Zhan, J.; He, J.; Day, C.; Lu, Y.; McPerson, G. L.; Piringer, G.; John, V. T. Reactivity characteristics of nanoscale zerovalent iron-silica composites for trichloroethylene remediation. *Environ. Sci. Technol.* **2008**, *42*, 4494–4499.

(12) Gu, C.; Jia, H. Z.; Li, H.; Teppen, J. B.; Boyd, A. S. Synthesis of highly reactive subnanosized zero-valent iron using smectite clay templates. *Environ. Sci. Technol.* **2010**, *44*, 4258–4263.

(13) Li, A.; Tai, C.; Zhao, Z.; Wang, Y.; Zhang, Q.; Jiang, G.; Hu, J. Debromination of decabrominated diphenyl ether by resin-bound iron nanoparticles. *Environ. Sci. Technol.* **2007**, *41*, 6841–6846.

(14) Li, J. F.; Lu, J. H.; Li, Y. M. Carboxylmethylcellulose/ bentonite composite gels: water sorption behavior and controlled release of herbicide. *J. Appl. Polym. Sci.* **2009**, *112*, 261–268.

(15) Li, J. F.; Li, Y. M.; Meng, Q. L. Removal of nitrate by zero-valent iron and pillared bentonite. *J. Hazard. Mater.* **2010**, *174*, 188–193.

(16) Yang, Z.; Xiao, O.; Chen, B.; Zhang, L.; Zhang, H.; Niu, X.; Zhou, S. Perchlorate adsorption from aqueous solution on inorganic-pillared bentonites. *Chem. Eng. J.* **2013**, *223*, 31−39.
(17) Li, Y. M.; Zhang, Y.; Li, J. F.; Zheng, X. M. Enhanced removal of pentachlorophenol by a novel composite: Nanoscale zero valent iron immobilized on organobentonite. *Environ. Pollut.* **2011**, *159*, 3744−3749.
(18) Li, Y.; Li, J.; Zhang, Y. Mechanism insights into enhanced Cr(VI) removal using nanoscale zerovalent iron supported on the pillared bentonite by macroscopic and spectroscopic studies. *J. Hazard. Mater.* **2012**, *227−228*, 211−218.
(19) Zhang, Y.; Li, Y. M.; Li, J. F.; Hu, L. J.; Zheng, X. M. Enhanced removal of nitrate by a novel composite: Nanoscale zero valent iron supported on pillared clay. *Chem. Eng. J.* **2011**, *171*, 526−531.
(20) Zhang, Y.; Li, Y. M.; Zheng, X. M. Removal of atrazine by nanoscale zero valent iron supported on organobentonite. *Sci. Total Environ.* **2011**, *409*, 625−630.
(21) Cheng, R.; Wang, J. L.; Zhang, W. X. Comparison of reductive dechlorination of p-chlorophenol using Fe^0 and nanosized Fe^0. *J. Hazard. Mater.* **2007**, *144*, 334−339.
(22) Gu, L.; Xu, J.; Lv, L.; Liu, B.; Zhang, H.; Yu, X.; Luo, Z. Dissolved organic nitrogen (DON) adsorption by using Al-pillared bentonite. *Desalination* **2011**, *269*, 206−213.
(23) Peng, X. J.; Luan, Z. K.; Chen, F. T.; Tian, B. H.; Jia, Z. P. Adsorption of humic acid onto pillared bentonite. *Desalination* **2005**, *174*, 135−143.
(24) Kumar, K. V.; Porkodi, K.; Rocha, F. Langmuir−Hinshelwood kinetics: A theoretical study. *Catal. Commun.* **2008**, *9*, 82−84.
(25) Oh, Y. J.; Song, H.; Shin, W. S.; Choi, S. J.; Kim, Y. H. Effect of amorphous silica and silica sand on removal of chromium(VI) by zero-valent iron. *Chemosphere* **2007**, *66*, 858−865.
(26) Powell, R. M.; Puls, R. W. Proton generation by dissolution of intrinsic or augmented aluminosilicate minerals for in situ contaminant remediation by zero-valence-state iron. *Environ. Sci. Technol.* **1997**, *31*, 2244−2251.
(27) Schinder, M.; Haethorne, F. C.; Freund, M. S.; Burns, P. C. XPS spectra of uranyl minerals and synthetic uranyl compounds. I: The U 4f spectrum. *Geochim. Cosmochim. Acta* **2009**, *73*, 2471−2487.
(28) O'Loughlin, E. J.; Kelly, S. D.; Kemner, K. M. An XAFS investigation of the interactions of U^{VI} with secondary mineralization products from the bioreduction of Fe^{III} oxides. *Environ. Sci. Technol.* **2010**, *44*, 1656−1661.
(29) O'Loughlin, E. J.; Kelly, S. D.; Cook, R. E.; Csencsits, R.; Kemner, K. M. Reduction of uranium(VI) by mixed iron(II)/iron(III) hydroxide (green rust): formation of UO_2 nanoparticles. *Environ. Sci. Technol.* **2003**, *37*, 721−727.
(30) Chakraborty, S.; Favre, F.; Banerjee, D.; Scheinost, A. C.; Mullet, M.; Ehrhardt, J. J.; Brendle, J.; Vidal, L.; Charlet, L. U(VI) Sorption and Reduction by Fe(II) Sorbed on Montmorillonite. *Environ. Sci. Technol.* **2010**, *44*, 3779−3785.
(31) Charlet, L.; Scheinost, A. C.; Tournassat, C.; Greneche, J. M.; Gehin, A.; Fernandez-Martinez, A.; Coudert, S.; Tisserand, D.; Brendle, J. Electron transfer at the mineral/water interface: Selenium reduction by ferrous iron sorbed on clay. *Geochim. Cosmochim. Acta* **2007**, *71*, 5731−5749.
(32) Jaisi, D. P.; Dong, H. L.; Plymale, A. E.; Fredrickson, J. K.; Zachara, J. M.; Heald, S.; Liu, C. X. Reduction and long-term immobilization of technetium by Fe(II) associated with clay mineral nontronite. *Chem. Geol.* **2009**, *264*, 127−138.